NIR Dyes Based on [M(R,R′timdt)$_2$] Metal-Dithiolenes: Additivity of M, R, and R′ Contributions To Tune the NIR Absorption (M = Ni, Pd, Pt; R,R′timdt = Monoreduced Form of Disubstituted Imidazolidine-2,4,5-trithione)

M. Carla Aragoni,[a] Massimiliano Arca,*[a] Tiziana Cassano,[b] Carla Denotti,[a] Francesco A. Devillanova,[a] Romina Frau,[a] Francesco Isaia,[a] Francesco Lelj,[c] Vito Lippolis,[a] Luigi Nitti,[b] Pina Romaniello,[c] Raffaele Tommasi,[b] and Gaetano Verani[a]

Keywords: S ligands / Nickel / Palladium / Platinum / Density functional calculations / Nonlinear optics

With the aim of preparing new dyes for Q-switching and/or mode-locking Nd-based lasers, such as Nd:YLF and Nd:YAG (emission wavelengths 1053 and 1064 nm, respectively), the syntheses of about 30 new neutral dithiolenemetal complexes belonging to the class [M(R,R′timdt)$_2$] have been carried out [M = Ni (**4a–c**; **4g–j**), Pd (**5a–j**), Pt (**6a–j**); R,R′timdt = monoreduced form of disubstituted imidazolidine-2,4,5-trithione]. The examination of the effects induced on the intense NIR absorption by changing M, R, and R′ has allowed for the recognition of the additive contributions ($\Delta\lambda$) of the central metal ion and of the substituents to the $\lambda_{max}^{M,R,R'}$ position of the NIR absorption maximum, which is in the region of 1000 nm. The high $\Delta\lambda$ values due to aromatic substituents have been elucidated by means of Hybrid-DFT calculations performed on the model compound [Ni(H$_2$timdt)(Ph,H-timdt)]. Both the $\lambda_{max}^{M,R,R'}$ values and the molar extinction coefficients vary with the solvent. Complex **5f** [M = Pd, R = *p*-F-C$_6$H$_4$, R′ = *m*,*m*,*p*-(MeO)$_3$-C$_6$H$_2$] shows that it has been possible to exactly match the emission wavelength of the Nd:YLF and Nd:YAG lasers in chloroform and toluene, respectively (by choosing the appropriate combination of metal ion and substituents). The highest extinction coefficient ever observed for a metal-dithiolene (120000 $M^{-1}\cdot cm^{-1}$ at 1034 nm in toluene) is also reported for complex **6g** [M = Pt, R = *p*-F-C$_6$H$_4$, R′ = naphthyl]. Time-resolved absorption dynamics measurements on **5f** have also been carried out by means of pump-probe experiments, with a picosecond Nd:YAG Q-switched and mode-locked laser.

Introduction

The tuning of specific molecular properties by means of chemical modifications is of current interest in material chemistry and engineering.[1] During the past years, the design of organic chromophores with specific optical properties has been made possible thanks to the discovery of well-defined structure-property relationships (SPRs).[2−4] Nevertheless, the relationships between the structural factors and the nonlinear optical properties of inorganic materials are still not well understood.[1,5] In particular, this applies to the search for materials which can be used in laser applications, such as Q-switching or mode-locking. In order to be exploited as saturable absorbers, dyes have to satisfy several criteria. In particular, (i) the fundamental absorption should exhibit a very high cross-section at the laser emission wavelength, (ii) no excited-state absorption should be present at the same wavelength, and (iii) the molecules should be very stable when exposed to light. Moreover, in order to prevent damage to laser optics, the dyes must be quite soluble in inert solvents. Most materials used in laser applications are based on organic substrates, but these are generally photochemically not as stable as required.

Bis-dithiolene complexes of d^8 metals have been used for Q-switching near-infrared (NIR) lasers since the early 1970s,[6−8] and have also been used as materials for molecular magnets, conductors, and superconductors.[9,10] These complexes exhibit a high degree of π-electron delocalization,[11−13] involving the organic framework as well as the metal center,[14] which confers peculiar and unique molecular properties, such as planarity, optical non-

[a] Dipartimento di Chimica Inorganica ed Analitica, Complesso Universitario di Monserrato, S. S.
554 bivio per Sestu, 09042 Monserrato (Cagliari), Italy
Fax: (internat.) + 39-070/675-4456
E-mail: marca@unica.it
[b] DETO, Dipartimento di Fisica and INFM,
Via G. Amendola 173, 70126 Bari, Italy
[c] Dipartimento di Chimica,
Via N. Sauro 85, 85100 Potenza, Italy

linearity,[15] high thermal and photochemical stabilities, along with the ability to have a variable charge, which in some cases can vary reversibly from −2 to +2. The possibility of applying dithiolenes to laser technology relies on the unique property that these complexes feature an intense Vis/NIR absorption in the neutral state, due to a singlet[16] $\pi \rightarrow \pi^*$ transition between the HOMO and LUMO,[17] at frequencies which depend on the nature of the substituents at the carbon atoms of the dithiolene moiety.[6] In particular, donor substituents shift the position of this absorption to energies lower[9,17] than those found in the dithiolenes which are derived from the edt ligand {[$M(edt)_2$]; edt = ethylenedithiolato, M = Ni (**1**), λ_{max} = 720 nm; M = Pd (**2**), λ_{max} = 785 nm; M = Pt (**3**), λ_{max} = 680 nm}.[18−20] Obviously, among the various dithiolenes, only a few compounds meet all the requirements. Since 1995,[21] a series of papers has reported on the synthesis, spectroscopic and structural characterization,[22−24] reactivity[25,26] and photophysical properties[27−29] of the new class of dithiolenes [$M(R,R'timdt)_2$] [R,R′timdt = disubstituted monoreduced imidazolidine-2,4,5-trithione; M = Ni (**4**), Pd (**5**), Pt (**6**)]. The most striking property of these dithiolenes is the unusually intense absorption at about 1000 nm, with extinction coefficients in chloroform as high as 80000 $M^{-1}\cdot cm^{-1}$. This absorption is assigned to a $\pi-\pi^*$ singlet transition and has been confirmed by TD-DFT calculations.[27,28] The application of these dithiolenes to Nd-based lasers,[21,27] such as Nd:YLF and Nd:YAG (emission wavelengths 1053 and 1064 nm, respectively), was prevented by their very low solubility. Therefore, it was necessary to look for new substituents, with the aim of both increasing the solubility, and of simultaneously shifting the position of the absorption to values as close as possible to the emission wavelengths of the Nd lasers.

Here we report on the syntheses of almost 30 new dithiolenes belonging to the title class. By referring to the NIR spectral properties of all the dithiolenes synthesized so far, the present work shows that there is an additive effect of the metal ion and of the substituents on the maximum NIR absorption wavelength, and that it is possible to quantify these contributions to the position of the NIR absorption band. In particular, the high contribution by the aromatic groups is elucidated on the basis of DFT calculations. The absorption saturation temporal dynamics of the dithiolene **5f**, which exactly matches the emission wavelength of the Nd:YLF and Nd:YAG lasers in chloroform and toluene, respectively, has been investigated using the picosecond pump-probe technique. The physical processes responsible for the dynamics have been explained using multi-level rate equations,[27,28] supported by relativistic time-dependent density functional calculations.

Results and Discussion

In order to apply [$M(R,R'timdt)_2$] dithiolenes successfully to Q-switch or mode-lock Nd-based lasers, two main goals were to be achieved: a) to significantly increase their solubility in common organic solvents, such as chloroform or dichloromethane; and b) to ensure that the wavelength of the maximum in the NIR absorption is as close as possible to the target laser emission wavelength. The change in the central metal ion and in the substituents R and R′ at the nitrogen atoms enables both objectives to be met. In fact, from the NIR spectra of the first series of synthesized Ni, Pd, and Pt complexes belonging to this class,[24] it could be seen that both the solubility and the position of the NIR absorption depend on the metal ion and on the R and R′ substituents; e.g., aromatic substituents shift the position of the absorption in the desired direction, however, the solubility in low-polar solvents is greatly reduced. With the aim of obtaining a satisfactory solubility, and in order to match the positions of the NIR absorption maxima with the laser emission wavelengths, several new [$M(R,R'timdt)_2$] dithiolenes have been prepared with alkyl and aryl substituents, in particular with the introduction of fluorine atoms or fluorine-rich groups into the phenyl ring.

Synthesis

According to the well-established route summarized in Scheme 1,[24] approximately 30 new Ni-, -Pd-, and Pt-dithiolenes, containing different types of substituents (**4a−c** and **4g−j**, **5a−j**, **6a−j** for Ni, Pd, and Pt, respectively), have been synthesized by the sulfuration of the corresponding disubstituted 2-thioxoimidazolidine-4,5-diones (**7a−j**) with Lawesson's reagent (**8**; 1,3,2,4-dithiadiphosphetane 2,4-disulfide).[30] Unfortunately, with the only exception of **4g**, the syntheses of the Ni complexes that are derived from the 2-thioxoimidazolidine-4,5-diones with a *p*-fluorophenyl substituent (**4d−f**) have not been successful. All the new compounds have been fully characterized by conventional methods, confirming the properties already reported for this class of neutral complexes.[23,24] In particular, the melting points are very high, generally over 250 °C, thus confirming their outstanding thermal stabilities. Among the synthesized dithiolenes, those with phenyl substituents are, in general, not very soluble. However, the solubility increases when naphthyl or *p*-CF_3O-C_6H_4 groups are present.

NIR-Spectroscopy

Effect of M, R, and R′

Considering the new dithiolenes and those previously reported,[24] the typical NIR absorption maximum in $CHCl_3$ ($\lambda_{max}^{M,R,R'}$) spans over 60 nm between 991 (M = Ni; R = R′ = Me) and 1053 nm (**5f**). The molar extinction coefficients in the same solvent are in some cases higher than the previously reported[24] maximum value of 80000 $M^{-1}\cdot cm^{-1}$. For example, among the new most soluble complexes, **6c**, **6g**, and **6h** have values of 91000, 105000, and 110000 $M^{-1}\cdot cm^{-1}$, respectively, which are by far the highest values ever reported for dithiolene complexes.

The qualitative observation that the $\lambda_{max}^{M,R,R'}$ values depend on both the central metal ion and the substituents R and R′ has now been quantified, due to the great number

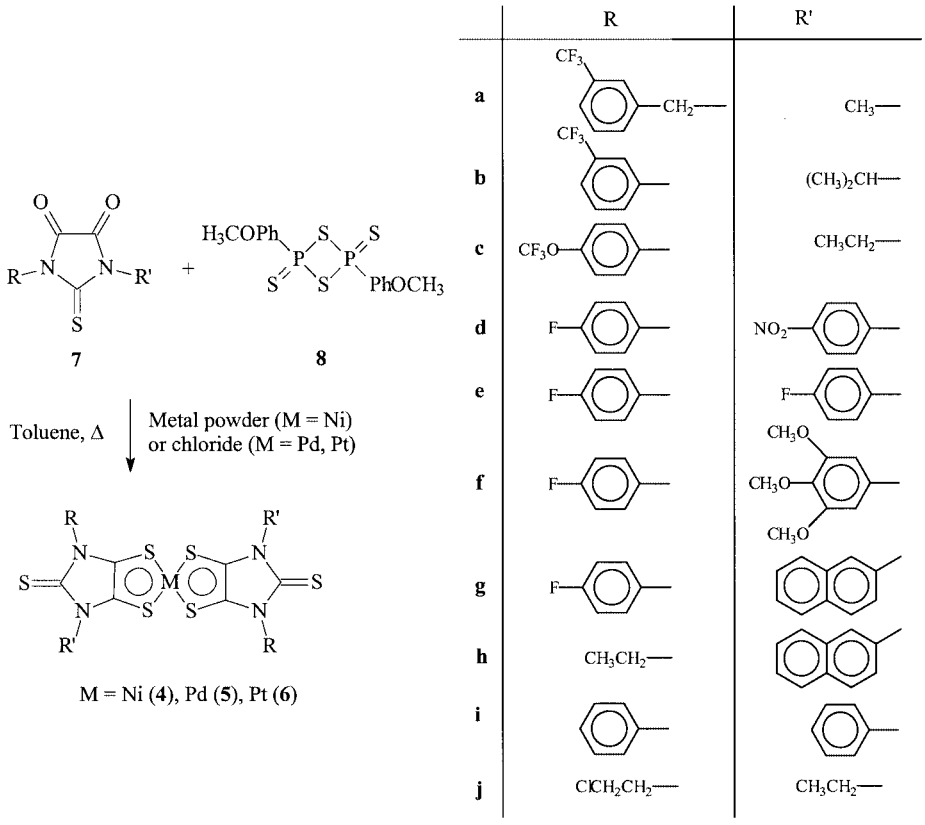

Scheme 1. Overall reaction path in the syntheses of dithiolenes **4**−**6**

(about 60) of synthesized dithiolenes, according to the relationship

$$\lambda_{max}^{M,R,R'} = \lambda_{max}^{Ni,Me,Me} + \Delta\lambda^{M} + \sum_{j=1}^{4}\Delta\lambda_{j}^{R}$$

where $\lambda_{max}^{Ni,Me,Me}$ represents the absorption wavelength recorded for [Ni(Me$_2$timdt)$_2$] ($\lambda_{max}^{Ni,Me,Me}$ = 991 nm), which can be considered the simplest member of this class of compounds. A least-squares fit (R = 0.97) of the experimental values listed in Table 1 has allowed for the evaluation of the contribution of the metal ion ($\Delta\lambda^{M}$) and of each substituent ($\Delta\lambda^{R}$). The goodness of such a regression (Figure 1) can be used to predict the absorption wavelength position of a particular dithiolene with a peculiar metal ion and substituent. As reported in Table 1, the central metal ion Pd confers a remarkable contribution ($\Delta\lambda^{Pd}$ = 20.59 nm) to $\lambda_{max}^{M,R,R'}$, compared with Ni and Pt ($\Delta\lambda^{M}$ = 0.00 and 1.62 nm for M = Ni and Pt, respectively). The bathochromic shift is influenced by the electron-releasing ability of the substituents; thus, for alkyl substituents, the shift increases with the length of the chain ($\Delta\lambda^{R}$ = 1.52, 1.86, 2.93, 3.72 nm for R = Et, *i*Pr, pentyl and nonyl, respectively) in agreement with an increasing $+I$ effect. The bathochromic effect due to the phenyl ring is more effective, and depends on the presence of groups bonded to the phenyl ring [$\Delta\lambda^{R}$ = 7.86, 5.36, 8.86 and 12.95 nm for R = phenyl, *p*-F-C$_6$H$_4$, *p*-Cl-C$_6$H$_4$, and *m*,*m*,*p*-(MeO)$_3$-C$_6$H$_2$, respectively]. Unexpectedly, the extension of π-aromaticity in the ligand (π-aromaticity extends from phenyl to naphthyl substituents) does not significantly increase the $\lambda_{max}^{M,R,R'}$ values ($\Delta\lambda^{R}$ = 7.86, 8.38 nm for R = phenyl, naphthyl, respectively).

Theoretical Calculations

The assignment of the intense low-energy Vis/NIR transition to a singlet π−π* HOMO−LUMO excitation,[16] peculiar to bis-dithiolenes, was also confirmed for [M(R,R′timdt)$_2$], based on Hybrid-DFT[24] and TD-DFT[28] calculations performed on the [M(H$_2$timdt)$_2$] complexes [M = Ni (**4^H**), Pd (**5^H**), Pt(**6^H**)], i.e. on the hypothetical complexes with four hydrogen atoms instead of the four organic substituents. These calculations accounted for the trends found on changing the central metal ion, not only in the [M(R,R′timdt)$_2$] complexes, but also in those derived from the edt ligand.[18−20,24] Since it is very interesting to understand the origin of the remarkable bathochromic shift observed in the presence of aromatic substituents, Hybrid-DFT calculations at the same level of theory as those carried out on **4^H**−**6^H** have now been extended to the mixed-ligand [Ni(H$_2$timdt)(H,Ph-timdt)] model complex (**9**, Figure 2), where a phenyl ring has been introduced as a substituent at the nitrogen atom of the nickel complex. In addition, in order to evaluate the influence of the ring orientation with respect to the molecular plane, the geometry was optimized at different frozen C(9)−N(13)−C(21)−C(22) dihedral angles (θ) correspond-

Table 1. Experimental NIR absorption maxima $\lambda_{exp}^{M,R,R'}$ [nm] for neutral [M(R,R′timdt)$_2$] dithiolenes, compared with the $\lambda_{max}^{M,R,R'}$ [nm] estimated on the basis of the additive coefficients $\Delta\lambda^M$ and $\Delta\lambda^R$: $\Delta\lambda^M$ = 0.00 (Ni), 20.59 (Pd), 1.62 (Pt) nm; $\Delta\lambda^R$ = 0.00 (Me), 1.52 (Et), 1.86 (*i*Pr), 2.93 (pentyl), 3.72 (nonyl), 2.72 ($ClCH_2CH_2$), 7.86 (Ph), 5.36 (*p*-F-C_6H_4), 8.86 (*p*-Cl-C_6H_4), 8.98 (*p*-O_2N-C_6H_4), 9.05 (*p*-MeO-C_6H_4), 8.01 (*p*-F_3CO-C_6H_4), 6.65 (*m*-F_3C-C_6H_4), 12.95 [*m*,*m*,*p*-$(MeO)_3$-C_6H_2], 8.38 (naphthyl) nm

M	R	R′	Ref.	$\lambda_{exp}^{M,R,R'}$	$\Delta\lambda^M + \sum_{i=1}^{4}\Delta\lambda_i^R$	$\lambda_{max}^{M,R,R'}$
Ni	Et	*p*-CF_3O-C_6H_4	[a] **(4c)**	1010	19.04	1010
Ni	Et	$ClCH_2CH_2$	[a] **(4j)**	1001	8.46	999
Ni	Et	Et	[b]	996	6.06	997
Ni	Et	naphthyl	[a] **(4h)**	1007	19.78	1011
Ni	Et	pentyl	[b]	998	8.89	1000
Ni	Et	Ph	[b]	1010	18.75	1010
Ni	*p*-F-C_6H_4	naphthyl	[a] **(4g)**	1019	27.48	1018
Ni	Me	*m*-F_3C-$C_6H_4CH_2$	[a] **(4a)**	992	2.72	994
Ni	Me	*p*-MeO-C_6H_4	[b]	1009	18.00	1009
Ni	Me	*p*-Cl-C_6H_4	[b]	1008	17.72	1009
Ni	Me	Me	[b]	991	0.00	991
Ni	Me	nonyl	[b]	996	7.43	998
Ni	Me	pentyl	[c]	997	5.86	997
Ni	Me	Ph	[c]	1010	15.72	1007
Ni	Me	*i*Pr	[b]	996	3.73	995
Ni	Ph	Ph	[a] **(4i)**	1023	31.44	1022
Ni	*i*Pr	*m*-F_3C-C_6H_4	[a] **(4b)**	1008	17.03	1008
Pd	Et	*p*-CF_3O-C_6H_4	[a] **(5c)**	1032	39.43	1030
Pd	Et	$ClCH_2CH_2$	[a] **(5j)**	1027	42.57	1034
Pd	Et	Et	[b]	1017	26.45	1017
Pd	Et	naphthyl	[a] **(5h)**	1033	40.17	1031
Pd	Et	pentyl	[b]	1019	29.28	1020
Pd	Et	Ph	[b]	1030	39.14	1030
Pd	*p*-F-C_6H_4	*m*,*m*,*p*-$(MeO)_3$-C_6H_2	[a] **(5f)**	1052	56.88	1048
Pd	*p*-F-C_6H_4	*p*-F-C_6H_4	[a] **(5e)**	1027	41.84	1033
Pd	*p*-F-C_6H_4	naphthyl	[a] **(5g)**	1047	47.87	1039
Pd	*p*-F-C_6H_4	*p*-O_2N-C_6H_4	[a] **(5d)**	1040	49.11	1040
Pd	Me	*m*-F_3C-$C_6H_4CH_2$	[a] **(5a)**	1017	23.11	1014
Pd	Me	*p*-MeO-C_6H_4	[b]	1030	38.39	1029
Pd	Me	*p*-Cl-C_6H_4	[b]	1030	38.11	1029
Pd	Me	Me	[b]	1010	20.39	1011
Pd	Me	*p*-O_2N-C_6H_4	[b]	1030	38.39	1029
Pd	Me	nonyl	[b]	1020	27.82	1019
Pd	Me	pentyl	[c]	1017	26.25	1017
Pd	Me	*i*Pr	[b]	1013	24.11	1015
Pd	Ph	Ph	[a] **(5i)**	1042	51.83	1043
Pd	*i*Pr	*m*-F_3C-C_6H_4	[a] **(5b)**	1028	37.42	1028
Pt	Et	*p*-F_3CO-C_6H_4	[a] **(6c)**	1010	20.51	1012
Pt	Et	$ClCH_2CH_2$	[a] **(6j)**	1006	9.94	1001
Pt	Et	Et	[b]	998	7.54	999
Pt	Et	naphthyl	[a] **(6h)**	1011	21.26	1012
Pt	Et	pentyl	[b]	1004	10.37	1001
Pt	Et	Ph	[b]	1012	20.22	1011
Pt	*p*-F-C_6H_4	*m*,*m*,*p*-$(MeO)_3$-C_6H_2	[a] **(6f)**	1025	37.96	1029
Pt	*p*-F-C_6H_4	*p*-F-C_6H_4	[a] **(6e)**	1015	22.93	1014
Pt	*p*-F-C_6H_4	naphthyl	[a] **(6g)**	1021	28.95	1020
Pt	*p*-F-C_6H_4	*p*-O_2N-C_6H_4	[b]	1021	30.20	1021
Pt	Me	*m*-F_3C-$C_6H_4CH_2$	[a] **(6a)**	994	4.19	995
Pt	Me	*p*-MeO-C_6H_4	[b]	1010	19.47	1010
Pt	Me	*p*-Cl-C_6H_4	[b]	1010	19.20	1010
Pt	Me	Me	[b]	993	1.47	992
Pt	Me	*p*-O_2N-C_6H_4	[b]	1010	19.47	1010
Pt	Me	nonyl	[b]	1001	8.91	1000
Pt	Me	pentyl	[c]	999	7.33	998
Pt	Me	*i*Pr	[b]	997	5.20	996
Pt	Ph	Ph	[a] **(6i)**	1022	32.91	1024
Pt	*i*Pr	*m*-F_3C-C_6H_4	[b]	1010	18.50	1010

[a] This work. [b] Taken from ref.[24] [c] Unpublished results.

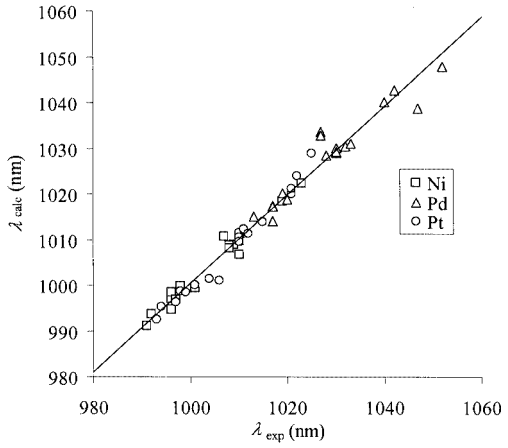

Figure 1. Linear correlation ($R = 0.97$) between experimental (λ_{exp}) and calculated (λ_{calc}) NIR absorption maxima wavelengths; λ_{calc} values have been evaluated by fitting with respect to the $\Delta\lambda^M$ and $\Delta\lambda^R$ parameters

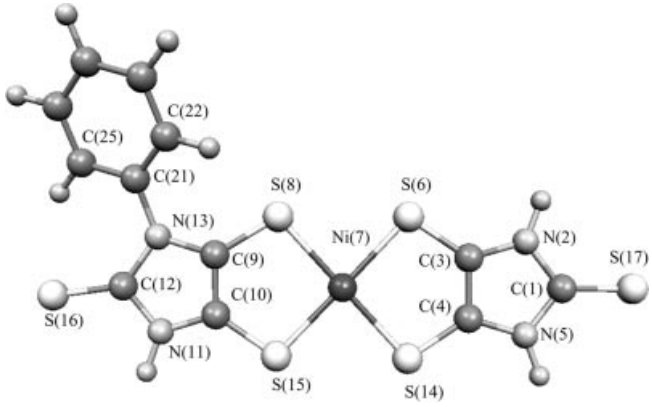

Figure 2. Drawing and atom numbering scheme of the model dithiolene **9**

ing to the rotation of the phenyl ring around the C(21)−N(13) bond. On passing from θ = 0° to θ = 180°, two local minima in the total electronic energy are found at 60 and 120°, respectively, while the maxima are found when the ring lies in the molecular plane (Table 2, Figure 3), the

Table 2. Relative total electronic DFT energy variation Δ*E*, Kohn−Shan energies for the HOMO and the LUMO (E^{HOMO} and E^{LUMO}, respectively), HOMO−LUMO energy gap ΔE, calculated for **9** at different torsional angles θ (0° ≤ θ ≤ 90°)

θ [°]	Δ*E* [kcal/mol][a]	E^{HOMO} [eV]	E^{LUMO} [eV]	ΔE [eV]
0	7.752	−5.287	−4.199	1.088
10	5.638	−5.271	−4.188	1.083
20	3.544	−5.249	−4.169	1.079
30	1.880	−5.225	−4.150	1.077
40	0.763	−5.206	−4.131	1.075
50	0.169	−5.187	−4.112	1.075
60	0.000	−5.170	−4.095	1.076
70	0.108	−5.157	−4.082	1.077
80	0.224	−5.148	−4.071	1.078
90	0.325	−5.146	−4.065	1.079

[a] ΔE = 1.078 eV for **4^H**.

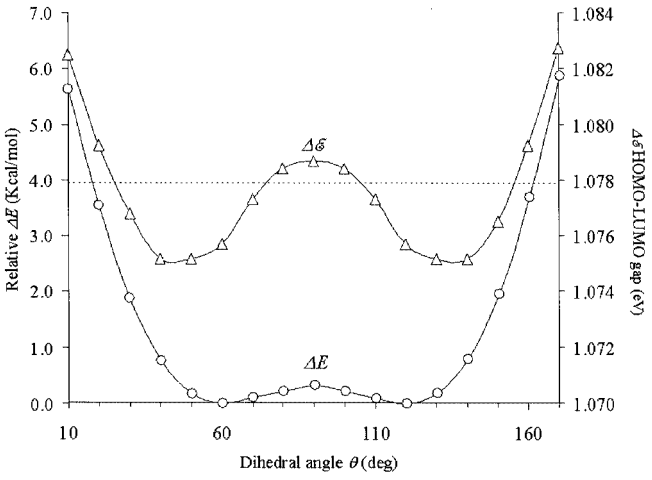

Figure 3. Relative total electronic energy variation Δ*E* (circles) and Kohn−Shan HOMO−LUMO energy gap ΔE (triangles) compared with the ΔE value calculated for **4^H** at the same level of theory (dotted line), calculated for **9** as a function of the phenyl rotation (θ)

difference between the two extremes being about 8 kcal/mol. The rotation around the C(21)−N(13) bond does not affect the nature of the main frontier orbitals. The calculated Kohn−Shan HOMO and LUMO are depicted in Figure 4. The former is a π-orbital extended over the whole molecule, with the contribution of the p_z atomic orbitals of all the atoms, with the exception of the metal center and the carbon atoms of the terminal thioxo groups. All the atoms contribute to the π*-LUMO; the metal ion is directly involved through its nd_{xz} atomic orbitals. In Figure 3, the differences between the HOMO and LUMO energies, ΔE, calculated by varying the dihedral angle θ (Table 2), are also reported and compared with the energy calculated[24] for **4^H** at the same level of theory. The minima in the HOMO−LUMO energy gap are found when the phenyl ring is twisted by about 45° with respect to the dithiolene molecular plane, a value which is close to those calculated for the total electronic energy minima. Therefore, at θ values corresponding to a total electronic energy lower than 1 kcal/mol (40° ≤ θ ≤ 140°), the HOMO−LUMO energy gap in **9** is lower than the gap calculated for **4^H**. This is in agreement with the NIR bathochromic shift measured in the presence of phenyl rings, and in general, of aromatic substituents. Contrary to our expectations, it should be

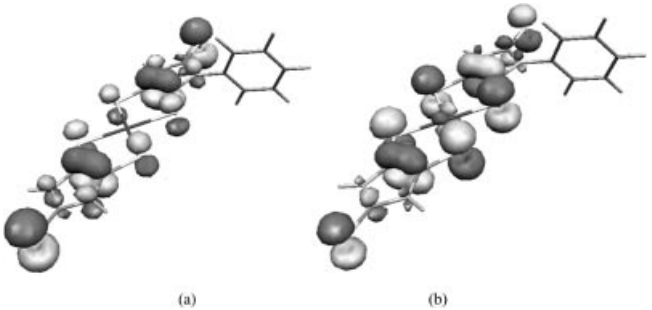

Figure 4. Sketches of Kohn−Shan HOMO (a) and LUMO (b) calculated for **9** at θ = 60° (contour value 0.05)

noted that such a shift is not directly due to the conjugation between the molecular electronic π-system and that of the phenyl ring, since the minima in the total electronic energy and those in the HOMO−LUMO energy gap, ΔE, are found at 45 and 60°, respectively. This also accounts for the $\Delta\lambda^{R}$ value of the naphthyl group (8.58 nm), which does not differ significantly from that estimated for the phenyl ring (7.86 nm).

Solvatochromic Effect

The UV/Vis/NIR spectra of the [M(R,R′timdt)$_2$] dithiolenes were recorded in solvents of varying polarity, ranging from CCl_4 (dielectric constant $\varepsilon_d = 2.2$) to dimethyl sulfoxide ($\varepsilon_d = 47.2$). As previously observed for different neutral nickel-dithiolenes,[31] both the $\lambda_{max}^{M,R,R'}$ and the molar extinction coefficient values depend on the nature of the solvents. Thus, the solvent is another factor that can be used to modulate the position of the NIR maximum. For solvents having dielectric constants of up to about 35, a continuous decrease in $\lambda_{max}^{M,R,R'}$ is observed on increasing ε_d; for solvents with high ε_d values (nitrobenzene, dimethylformamide, dimethyl sulfoxide: $\varepsilon_d = 35.7, 38.3, 47.2$) the trend is roughly reversed. This does not depend on the nature substituents R and R′, since it has been observed for all dithiolenes, and the change in the solvent does not affect the trend in $\Delta\lambda^{R}$: consequently, the λ_{max} values recorded in different solvents are linearly correlated (see Figure 5 for chloroform and toluene). The values recorded for [Pt(naphthyl,*p*-F-C_6H_4-timdt)$_2$] (**6g**) and [Pt(pentyl,Et-timdt)$_2$] are reported as an example in ref.[32], and in Figure 6 the NIR spectra of **6g** recorded in MeCN, $CHCl_3$, and toluene are superimposed (λ_{max}^{6g} = 1002, 1019 and 1034 in MeCN, $CHCl_3$ and toluene, respectively). As can be seen, the bathochromic shift is accompanied by an increase in the absorption extinction coefficients (90000, 105000 and 120000 $M^{-1}\cdot cm^{-1}$ in MeCN, $CHCl_3$, and toluene, respectively). It is worth noting that one of the proposed goals has been reached, since the NIR absorption maxima of **5f** in chloroform and toluene exactly match the emission wavelengths of the Nd:YLF and Nd:YAG lasers.

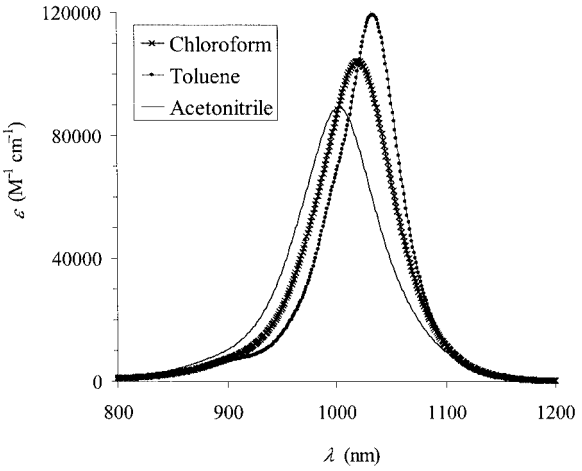

Figure 6. Vis/NIR spectra of **6g** ($c = 1.51 \times 10^{-5}$ M) recorded in acetonitrile, chloroform, and toluene

Photophysical Measurements

The thermal and photochemical stabilities of [Ni(*i*Pr$_2$-timdt)$_2$] had been previously tested in CH_2Cl_2 solution under the action of the FT-Raman spectrometer (0.5 W; 24 h).[22] Since an actual application implies much higher energies, the three dithiolenes **4c**−**6c** were dispersed in polythene pellets and exposed to the action of an Nd:YAG Q-switched mode-locked laser delivering 30-ps (FWHM) pulses at a 10 Hz repetition rate (λ_{em} = 1064 nm) for 9 h (324000 shots, power density 110 MW/cm^2). A comparison of the transmittance before and after the exposure reveals no change. The same test was performed on a commercially available Q-switching dye,[33] which showed a 30% decrease

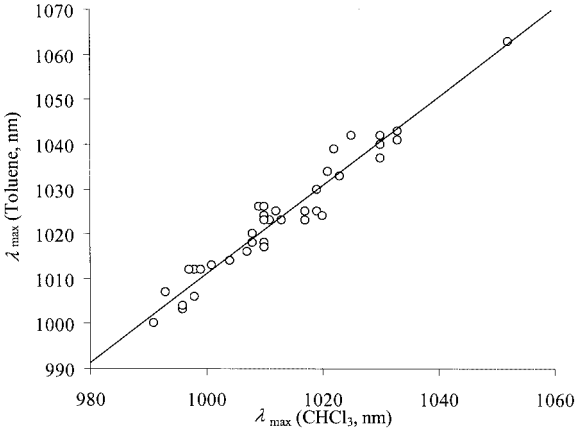

Figure 5. Linear relationship between the λ_{max} values found in chloroform and in toluene for Ni-, Pd-, and Pt-dithiolenes (R = 0.94)

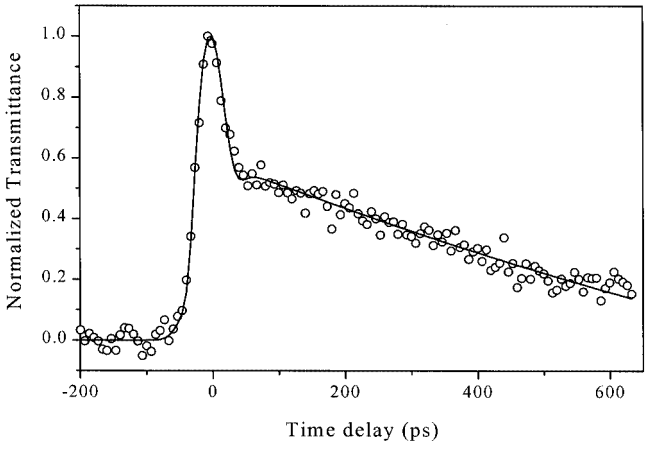

Figure 7. Experimental $\Delta T/T$ (dots) measured as a function of the pump-probe time delay in a chloroform solution of **5f** (λ = 1064 nm); the solid line is the least-squares fit of the experimental data

in transmittance after exposure for 1 h. The intense absorption of complex **5f** in toluene at the exact emission wavelength of the Nd:YAG laser suggested the investigation of its absorption saturation properties in this spectral region. Unfortunately, the low solubility in this solvent prevented pump-probe measurements, which were therefore performed in chloroform solution. The experimental results are reported in Figure 7. A fast increase in the transient normalized transmittance $\Delta T/T$ is observed, followed by a decay similar to those found[27] in other dithiolenes belonging to the same series. It has been shown that the decay depends on both the central metal ion and the substituents R and R′.[27] Based on TD-DFT calculations performed on the model complexes $\mathbf{4^H}-\mathbf{6^H}$, the six-level model reported in Figure 8 was proposed to account for the absorption dynamics.[27,28] According to this model, excitation from the ground state S_0 to the first dipole-allowed state S_2 occurs, which can decay to S_1. Since the transition to S_0 is dipole-forbidden, decay from S_1 to T_1 occurs through intersystem crossing. In addition, absorption from S_1 and T_1 to higher excited states S_n and T_k, resonant with the $S_0 \rightarrow S_2$ excitation, may be allowed. The numerical solution of the first-order differential equations reported in Figure 8 allows a least-squares fit of the experimental data (solid lines in Figure 7). The measured signal recovery that corresponds to the recovery of the absorption saturation, exhibits two components with different temporal dynamics. The fast decay is almost time-resolution-limited, and has essentially been assigned to the $S_2 \rightarrow S_1$ transition ($\tau_{32} \approx 4$ ps). On the contrary, the slower component decreases with a time constant ($\tau_{25} \approx 122$ ps) that is roughly inversely proportional to the spin-orbit coupling constant for the metal ion, indicating a large contribution of the intersystem crossing process $S_1 \rightarrow T_1$, to dynamics at long time delays. It should be mentioned that the absorption cross-sections for the $S_1 \rightarrow S_n$ and $T_1 \rightarrow T_k$ transitions are proportional to those relating to $S_0 \rightarrow S_2$, through γ_1 and γ_2 (see Figure 8), which have been considered as fitting parameters.

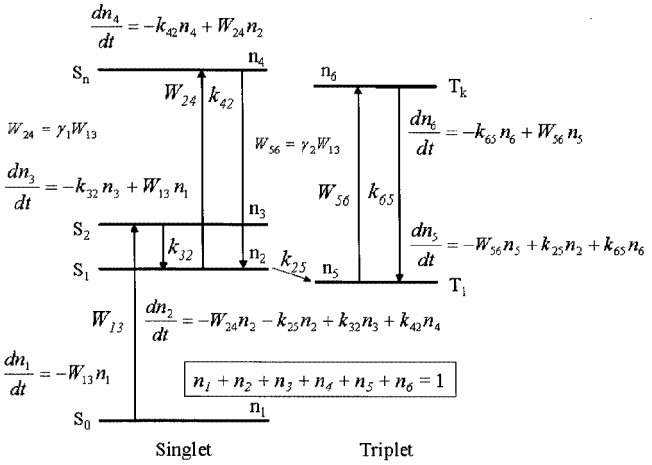

Figure 8. Scheme of the six-level model for the investigated complexes; the equations used as a model for the fitting of the pump-probe experiments are also reported; for **5f**, the main fit parameters are: $\tau_{32} = 4$ ps, $\tau_{25} = 122$ ps; $\gamma_1 = 1.9$; $\gamma_2 = 1.9$

Conclusions

The very high thermal and photochemical stabilities accompanied by the unprecedented intensities in the NIR absorption around 1000 nm show that the [M(R,R′timdt)$_2$] class of neutral dithiolenes is among the most promising classes of molecular materials for NIR laser applications. In addition, this class of complexes shows another interesting advantage compared with other dithiolenes, such as those derived from the dmit ligand, since a never-ending number of compounds can be synthesized by structurally modifying the substituents R and R′. Thus, the change in the central metal ion and the introduction of suitable polar groups in the substituents R and R′, along with the choice of a suitable solvent, allowed us to overcome solubility problems, as well as to modify the position of the NIR absorption maximum. In fact, the additivity of the contributions $\Delta\lambda^M$ and $\Delta\lambda^R$ in determining the $\lambda_{max}^{M,R,R'}$ position, accompanied by the solvatochromic effect depending on the dielectric constant of the solvent, allows for the tuning of the value of $\lambda_{max}^{M,R,R'}$ in a fairly wide range of wavelengths. Among the dithiolenes reported in this paper, compound **5f** [M = Pd, R = *p*-F-C$_6$H$_4$, and R′ = *m*,*m*,*p*-(MeO)$_3$-C$_6$H$_2$] matches the emission wavelengths of the Nd:YLF and Nd:YAG lasers exactly in chloroform and toluene, respectively. Moreover, the influence of the solvent on the molar extinction coefficient has allowed for the measurement of a value of 120000 $M^{-1}\cdot cm^{-1}$ for compound **6g** in toluene, the highest value ever encountered for a dithiolene complex. Through DFT calculations, it had been demonstrated that the metal ion contributes to the Kohn−Shan LUMO through its nd_{xy} atomic orbital (n = 3, 4, 5 for Ni, Pd, Pt), which depends on n. In this study, the DFT calculations have shown that the effect of the substituents arises mainly as a result of the inductive and/or steric factors, and not as a result of the extension of the π-aromaticity of the dithiolene system to the substituents, thus justifying the similar $\Delta\lambda^R$ contributions estimated for the phenyl and naphthyl groups. Finally, the behavior of these complexes as saturable absorbers has been proven, and the picosecond saturation dynamics for compound **5f** has been studied by a pump-probe technique, supporting future applications in the field of Nd-based lasers.

Experimental Section

Procedures and Methods: All solvents and reagents were Aldrich products used as purchased. All operations were carried out under dry nitrogen. The purity of each compound has been checked by CHNS and TLC analyses. Elemental analyses were performed with a FISONS EA-1108 CHNS-O instrument. FT-IR and FT-Raman spectra were collected as previously reported.[23,24] UV/Vis/NIR spectra were recorded using a 1-cm path-length cell, with a Varian Cary 5 spectrophotometer at 20 °C in a thermostatted compartment.

Disubstituted 2-Thioxoimidazolidine-4,5-diones 7a−j: These products were prepared according to literature methods by treating an

appropriate *N*,*N*′-dialkylthiourea or *N*-alkyl-*N*′-arylthiourea with oxalyl chloride in a CH_2Cl_2 solution,[23] and were recrystallized from CH_2Cl_2 or diethyl ether.

[Ni(R,R′timdt)$_2$] (4a−j): As previously pointed out,[24] both nickel powder and nickel chloride can be used in these syntheses, although higher yields are generally obtained starting from the metal powder. A general synthesis consists of refluxing the disubstituted 2-thioxoimidazolidine-4,5-dithione **7a−j** (about 5 mmol) with a slight excess (about 10%) of Lawesson's reagent (**8**) in 100 mL of previously degassed toluene for a time varying between 20 min and 1 h, depending on the substituents. After concentration of the reaction mixture, EtOH was added to lower the solubility of the complex and the dithiolene was filtered off. Starting from imidazolidine **7d−f**, the formation of the dithiolene complexes has not been proven. Yields % (mg, starting from 5 mmol of the corresponding 2-thioxoimidazolidine-4,5-dione): **4a**, 14 (255); **4b**, 15 (283); **4c**, 11 (209); **4g**, 8 (165); **4h**, 11 (190); **4i**, 5 (86); **4j**, 20 (282). Nickel-dithiolenes were recrystallized from chloroform/ethanol mixtures.

[Pd(R,R′timdt)$_2$] (5a−j): Compounds **5a−j** were synthesized according to the previously described procedure,[23,24] starting from compounds **7a−g** and using $PdCl_2$. Yields % (mg, starting from 5 mmol of the corresponding 2-thioxoimidazolidine-4,5-dione): **5a**, 42 (814); **5b**, 25 (502); **5c**, 18 (363); **5d**, 17 (381); **5e**, 21 (424); **5f**, 35 (834); **5g**, 22 (480); **5h**, 18 (333); **5i**, 48 (882); **5j**, 20 (306).

[Pt(R,R′timdt)$_2$] (6a−g): The syntheses of **6a−g** were very similar to those for the Pd analogues, starting from $PtCl_2$ instead of $PdCl_2$. Yields % (mg, starting from 5 mmol of the corresponding 2-thioxoimidazolidine-4,5-dione): **6a**, 32 (691); **6b**, 17 (379); **6c**, 24 (538); **6d**, 22 (493); **6e**, 21 (470); **6f**, 38 (990); **6g**, 33 (794); **6h**, 4 (83); **6i**, 66 (1360); **6j**, 65, (1139).

Elemental analyses of all synthesized dithiolenes correspond to the expected values.

Photophysical Measurements: A saturated solution of complex **5f** in chloroform was filtered and placed in a 1-mm quartz optical cell. The temporal dynamics of the saturable absorption was investigated using a picosecond time-resolved pump-probe technique. The ps Nd:YAG laser beam was divided into two parts using a beam splitter to create the pump and probe pulses. The pump beam was focused on a spot ca. 200 μm in diameter, in order to obtain a peak irradiance of about 20 GW/cm^2. The probe beam was focused on a smaller spot (ca. 50 μm) to reduce the effect of excitation spatial inhomogeneity, and its peak irradiance was always kept at about 0.1% of that of the pump. All the experiments were performed at $T = 295$ K. The experimental data were fitted according to a previously outlined procedure.[27]

Computations: Quantum chemical calculations were carried out by using the commercially available suite of programs Gaussian 98 package.[34] Density functional calculations (DFT)[35,36] regarding the model dithiolene **9** were performed using the hybrid Becke3LYP functional (which uses a mixture[37] of Hartree−Fock and DFT exchange, along with DFT correlation, the Lee−Yang−Parr correlation functional,[38] together with Becke's gradient correction[39]). The basis set for all calculations was the Schafer, Horn, and Ahlrichs pVDZ basis[40] for C, H, N, and S, while for Ni, Hay−Wadt LANL2DZ basis sets together with ECP sets[41] were employed. After scanning the potential energy surface by rotating the phenyl ring in dithiolene **9** by 10° between 0 and 180°, single optimization calculations were performed at each rotational step to calculate the orbital compositions and the Kohn−Shan orbital energies. All the results were elaborated with the Molekel 4.2 program.[42] The values of $\Delta\lambda^M$ and $\Delta\lambda^R$ were estimated by an iterative least-squares fit minimizing the squared sum

$$\sum_{i}^{N}\left|\lambda_{max}^{M,R,R'}(i)-\lambda_{max}^{Ni,Me,Me}-\Delta\lambda^{M(i)}-\sum_{j}^{4}\Delta\lambda^{R(i,j)}\right|^2$$

of the differences between experimental $\lambda_{max}^{M,R,R'}$ and estimated values for each of the N synthesized dithiolenes, where $\lambda_{max}^{Ni,Me,Me}$ is the NIR absorption wavelength recorded for [Ni(Me$_2$timdt)$_2$].

Acknowledgments

This project was carried out as part of a MIUR (Ministero dell'Istruzione dell'Università della Ricerca) project. CINECA (Centro Interuniversitario Nord Est Calcolo Automatico) is also acknowledged for computational facilities. We wish to thank Dr. Antonio Masello for the help in the syntheses of compounds **4j−6j**.

[1] K. Base, M. T. Tierney, A. Fort, J. Muller, M. W. Grinstaff, *Inorg. Chem.* **1999**, *38*, 287−289.
[2] S. R. Marder, C. B. Gorman, F. Meyers, J. W. Perry, G. Bourhill, J. L. Bredas, B. M. Pierce, *Science* **1994**, *265*, 632−635.
[3] S. R. Marder, D. N. Beratan, L. T. Cheng, *Science* **1991**, *252*, 103−106.
[4] F. Meyers, S. R. Marden, B. M. Pierce, J. L. Bredas, *J. Am. Chem. Soc.* **1994**, *116*, 10703−10714.
[5] S. D. Cummings, L.-T. Cheng, R. Eisemberg, *Chem. Mater.* **1997**, *9*, 440−450.
[6] U. T. Mueller-Westerhoff, B. Vance, D. I. Yoon, *Tetrahedron* **1991**, *47*, 909−932.
[7] U. T. Mueller-Westerhoff, K. H. Drexhage, *IEEE J. Quantum Electron. QE-8* **1972**, 759−763.
[8] U. T. Mueller-Westerhoff, K. H. Drexhage, US Patent 3,743,964, **1973**.
[9] P. Cassoux, *Coord. Chem. Rev.* **1999**, *185−186*, 213−232.
[10] E. Canadell, *Coord. Chem. Rev.* **1999**, *185−186*, 629−651.
[11] G. N. Schrauzer, V. P. Mayweg, *J. Am. Chem. Soc.* **1966**, 3235−3242.
[12] D. C. Olson, V. P. Mayweg, G. N. Schrauzer, *J. Am. Chem. Soc.* **1966**, 4876−4882.
[13] M. D. Ward, J. A. McCleverty, *J. Chem. Soc., Dalton Trans.* **2002**, 275−288.
[14] R. Williams, E. Billig, J. H. Waters, H. B. Grey, *J. Am. Chem. Soc.* **1966**, *88*, 43−50.
[15] S. N. Oliver, S. V. Kershaw, A. E. Underhill, C. A. S. Hill, A. Charlton, *Nonlinear Opt.* **1995**, *10*, 87−99.
[16] W. L. Tan, W. Ji, J. L. Zuo, J. F. Bai, X. Z. You, J. H. Lim, S. Yang, D. J. Hagan, E. W. Van Stryland, *Appl. Phys. B* **2000**, *70*, 809−812.
[17] U. T. Mueller-Westerhoff, B. Vance, in *Comprehensive Coordination Chemistry*, 1st ed., Pergamon Press, Oxford, England, **1987**, vol. 2, p. 595−631.
[18] K. W. Browall, T. Bursh, L. V. Interrante, *Inorg. Chem.* **1972**, *11*, 1800−1806.
[19] K. W. Browall, L. V. Interrante, *J. Coord. Chem.* **1973**, *3*, 27−38.
[20] G. N. Schrauzer, V. P. Mayweg, *J. Am. Chem. Soc.* **1965**, *87*, 3585−3592.
[21] F. Bigoli, P. Deplano, F. A. Devillanova, V. Lippolis, P. J. Lukes, M. L. Mercuri, M. A. Pellinghelli, E. F. Trogu, *J. Chem. Soc., Chem. Commun.* **1995**, 371−372.
[22] F. Bigoli, P. Deplano, F. A. Devillanova, J. R. Ferraro, V. Lippolis, P. J. Lukes, M. L. Mercuri, M. A. Pellinghelli, E. F. Trogu, J. M. Williams, *Inorg. Chem.* **1997**, *36*, 1218−1226.
[23] M. Arca, F. Demartin, F. A. Devillanova, A. Garau, F. Isaia, F. Lelj, V. Lippolis, S. Pedraglio, G. Verani, *J. Chem. Soc., Dalton Trans.* **1998**, 3731−3736.

[24] M. C. Aragoni, M. Arca, F. Demartin, F. A. Devillanova, A. Garau, F. Isaia, F. Lelj, V. Lippolis, G. Verani, *J. Am. Chem. Soc.* **1999**, *121*, 7098−7107.
[25] F. Bigoli, P. Deplano, M. L. Mercuri, M. A. Pellinghelli, G. Pintus, E. F. Trogu, G. Zonnedda, H. H. Wang, J. Williams, *Inorg. Chim. Acta* **1998**, *273*, 175−183.
[26] F. Bigoli, S. Curreli, P. Deplano, L. Leoni, M. L. Mercuri, M. A. Pellinghelli, A. Serpe, E. F. Trogu, *J. Chem. Soc., Dalton Trans.* **2002**, 1985−1991.
[27] T. Cassano, R. Tommasi, L. Nitti, M. C. Aragoni, M. Arca, C. Denotti, F. A. Devillanova, F. Isaia, V. Lippolis, F. Lelj, P. Romaniello, *J. Chem. Phys.*, in press.
[28] P. Romaniello, M. C. Aragoni, M. Arca, T. Cassano, C. Denotti, F. A. Devillanova, F. Isaia, F. Lelj, V. Lippolis, R. Tommasi, *J. Phys. Chem.*, submitted.
[29] M. C. Aragoni, M. Arca, T. Cassano, C. Denotti, F. A. Devillanova, F. Isaia, V. Lippolis, D. Natali, L. Nitti, M. Sampietro, R. Tommasi, G. Verani, *Inorg. Chem. Commun.* **2002**, *5*, 869−872.
[30] S. Sheibe, B. J. Pedersen, S.-O. Lawesson, *Bull. Soc. Chim. Belg.* **1978**, *87*, 229−240.
[31] W. Freyer, *J. Prakt. Chem.* **1986**, *328*, 253−260.
[32] NIR absorption maxima [nm] recorded for [Pt(naphthyl,*p*-F-C_6H_4-timdt)$_2$] and [Pt(pentyl,Et-timdt)$_2$] in various solvents (dielectric constants ε_d in paretheses): THF (7.52) 1024, 1004; CCl_4 (2.24) 1032, 1013; benzene (2.28) 1034, 1015; *p*-xylene (2.4) 1034, 1014; toluene (2.4) 1034, 1015; $CHCl_3$ (4.8) 1021, 1004; CH_2Cl_2 (9.08) 1017, 1001; MeCN (37.5) 1002, 986; ethyl acetate (6.02) 1015, 996; MeOH (32.6) 1001, 985; EtOH (24.3) 1009, 994; 1,4-dioxane (2.2) 1024, 1005: 1,2-dichloroethane (16.7) 1022, 1006; DMF (38.3) 1027, 1006; DMSO (47.2) 1036, 1015; nitrobenzene (35.7) 1037, 1009. The two sets of data are linearly correlated ($R = 0.95$).
[33] 6-Methyl-8-[5-(6-methyl-2,4-diphenyl-6,7-dihydro-5*H*-chromen-8-yl)penta-2,4-dienylidene]-2,4-diphenyl-5,6,7,8-tetrahydro-2*H*-chromenium perchlorate.
[34] M. J. Frisch, G. W. Trucks, H. B. Schlegel, G. E. Scuseria, M. A. Robb, J. R. Cheeseman, V. G. Zakrzewski, J. A. Montgomery, R. E. Stratmann, J. C. Burant, S. Dapprich, J. M. Millam, A. D. Daniels, K. N. Kudin, M. C. Strain, O. Farkas, J. Tomasi, V. Barone, M. Cossi, R. Cammi, B. Mennucci, C. Pomelli, C. Adamo, S. Clifford, J. Ochterski, G. A. Petersson, P. Y. Ayala, Q. Cui, K. Morokuma, D. K. Malick, A. D. Rabuck, K. Raghavachari, J. B. Foresman, J. Cioslowski, J. V. Ortiz, B. B. Stefanov, G. Liu, A. Liashenko, P. Piskorz, I. Komaromi, R. Gomperts, R. L. Martin, D. J. Fox, T. Keith, M. A. Al-Laham, C. Y. Peng, A. Nanayakkara, C. Gonzalez, M. Challacombe, P. M. W. Gill, B. G. Johnson, W. Chen, M. W. Wong, J. L. Andres, M. Head-Gordon, E. S. Replogle, J. A. Pople, *Gaussian 98* (Revision A.7), Gaussian, Inc., Pittsburgh, PA, **1998**.
[35] E. S. Kryachko, E. V. Ludeña, *Energy Density Function Theory of Many Electron Systems*, Kluwer Academic Publisher, Dortrecht, Boston, **1990**.
[36] B. Miehlich, A. Savin, H. Stoll, H. Preuss, *Chem. Phys. Lett.* **1989**, *157*, 200−206.
[37] A. D. Becke, *J. Chem. Phys.* **1993**, *98*, 1372−1377.
[38] C. Lee, W. Yang, R. G. Parr, *Phys. Rev. B* **1988**, *37*, 785−789.
[39] A. D. Becke, *J. Chem. Phys.* **1993**, *98*, 5648−5652.
[40] A. Schafer, H. Horn, R. Ahlrichs, *J. Chem. Phys.* **1992**, *97*, 2571−2577.
[41] P. J. Hay, W. R. Wadt, *J. Chem. Phys.* **1985**, *82*, 270−298.
[42] S. Potmann, H. P. Lüthi, *Chimia* **2000**, *54*, 766−769.

Received November 11, 2002

